Demography of the endangered North Atlantic right whale

Masami Fujiwara & Hal Caswell

Biology Department, MS34, Woods Hole Oceanographic Institution, Woods Hole, Massachusetts, USA

Northern right whales (*Eubalaena glacialis*) were formerly abundant in the northwestern Atlantic, but by 1900 they had been hunted to near extinction. After the end of commercial whaling the population was thought to be recovering slowly; however, evidence indicates that it has been declining since about 1990 (ref. 1). There are now fewer than 300 individuals, and the species may already be functionally extinct[2,3] owing to demographic stochasticity or the difficulty of females locating mates in the vast Atlantic Ocean (Allee effect[4]). Using a data set containing over 10,000 sightings of photographically identified individuals we estimated trends in right whale demographic parameters since 1980. Here we construct, using these estimates, matrix population models allowing us to analyse the causes of right whale imperilment. Mortality has increased, especially among mother whales, causing declines in population growth rate, life expectancy and the mean lifetime number of reproductive events between the period 1980–1995. Increased mortality of mother whales can explain the declining population size, suggesting that the population is not doomed to extinction as a result of the Allee effect. An analysis of extinction time shows that demographic stochasticity has only a small effect, but preventing the deaths of only two female right whales per year would increase the population growth rate to replacement level.

Conservation biology uses population models to assess population performance, to diagnose the causes of poor performance, to prescribe management interventions, and to make prognoses of population viability (see chapter 18 of ref. 5). We have developed a stage-structured matrix population model[5–7] that addresses all four of these tasks. This matrix model uses the life cycle shown in Fig. 1 (a similar model has been successfully applied to a killer whale population[8]). The parameters in the matrix model were defined by a series of statistical models, the parameters of which were estimated by applying stage-structured mark–recapture analysis[5,9,10] to photographic identification data collected by the New England Aquarium (NEA)[11]. The best model was selected using Akaike Information Criteria (AIC)[12–14] (see Methods).

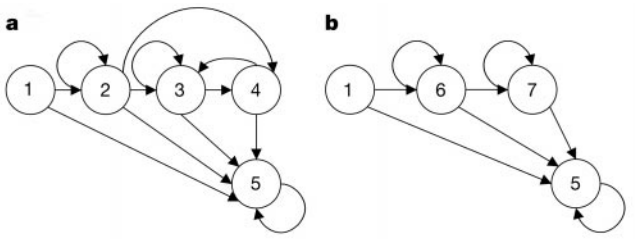

Figure 1 Life cycle graphs of female (**a**) and male (**b**) right whales. Numbers represent different stages: 1, calf; 2, immature female; 3, mature female; 4, mature females with newborn calves (mothers); 5, dead; 6, immature male; 7, mature male. Each arrow represents a possible transition in stage from one year to the next; the arrows going to stage 5 represent stage-specific mortalities. A calf is an individual that was sighted along with its mother. An immature is an individual known to be less than 9 years old. Mature individuals are known to be at least 9 years old, or in the case of females, have been sighted previously with a calf. Mothers are females that are sighted with a newborn offspring. If the sex of an individual is unknown, we assume it has an equal chance of being either female or male, as our data contain almost equal numbers of individuals (141 and 143) known to be female and male, respectively. Maturity status (whether an individual is immature or mature) is unknown in 22% of sightings. When maturity status was unknown, we estimated the probability that the individual was immature (0.30 for males, 0.87 for females) using the method described in ref. 10. These probabilities were used in stage-assignment matrices[10] for likelihood calculations.

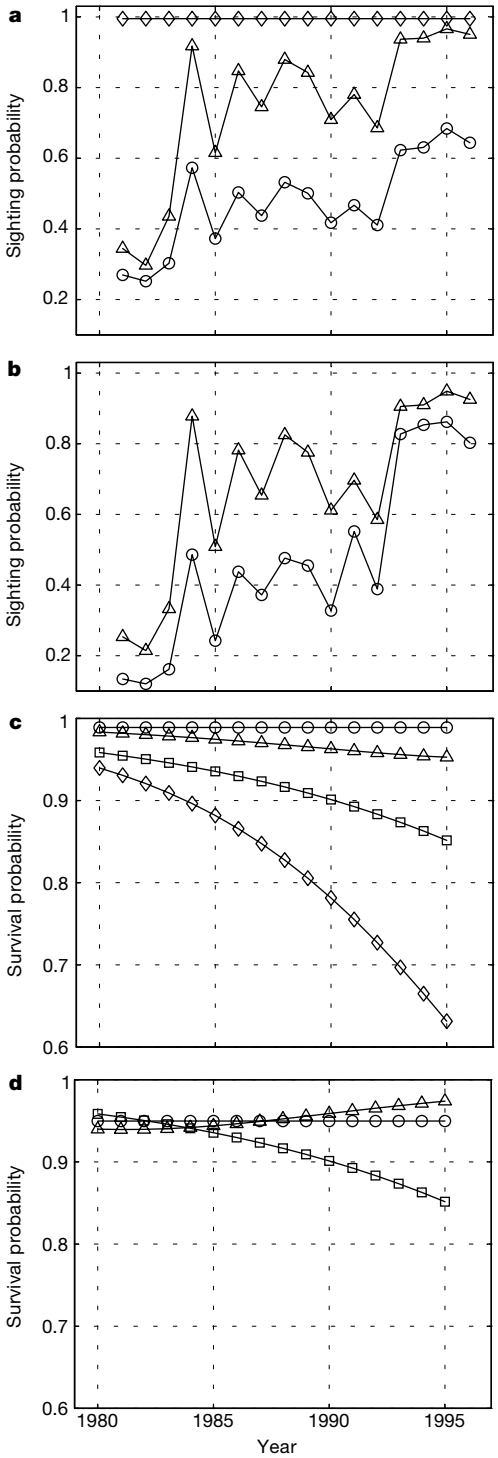

Figure 2 Stage-specific sighting and survival probabilities for males and females. **a**, **b**, Stage-specific sighting probabilities of the best model (M_2) for females (**a**) and males (**b**). **c**, **d**, Stage-specific survival probabilities (M_2) for females (**c**) and males (**d**). Squares, calf; triangles, immature; circles, mature; diamonds, mothers.

© 2001 Macmillan Magazines Ltd

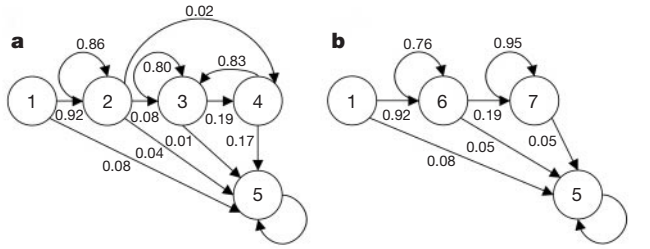

Figure 3 Constant transition probabilities estimated using the best sighting model (M_1). Life cycle graphs of female (**a**) and male (**b**) right whales. The numbers in the circles are the same as in Fig. 1.

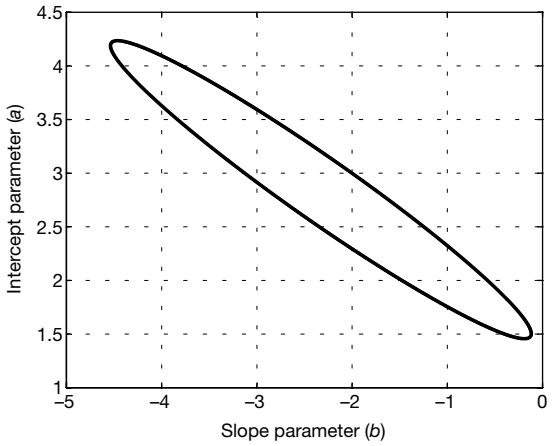

Figure 4 Joint 95% profile likelihood confidence region for the logistic parameters of survival probability of mothers.

In the resulting model, the sighting probability of most stages depends on both northern and southern effort levels (Fig. 2a, b; see Methods for definition). This is consistent with a previous study[1], which found a significant correlation between total effort and sighting probability in a simpler model that did not distinguish sex or stages. In contrast to other stages, mothers have a consistently high sighting probability (Fig. 2a). This suggests that they are easier to sight than other stages, and that the survey effort in the two regions has been sufficient to detect almost all births with high probability.

Using the best sighting probability model, we estimated two transition models. One model assumed time-invariant transition probabilities (M_1) and the other was the best time-varying model according to the AIC criterion (M_2). The time-invariant model (M_1, $b_{ji} = 0$ for all j and i in equation (2)) gives a weighted, time-averaged picture of transition probabilities. In this model, survival probability is low for calves, higher for immature and mature females and much lower for mothers (Fig. 3). According to the best time-varying model (M_2), the transition probabilities of mature females and males have been constant, whereas the other stages have transition probabilities that change with time. The survival probability of mothers shows the most pronounced decline over time (Fig. 2c, d). This trend is statistically significant, as the slope parameter (b_{34}) in the polychotomous logistic function (equation (2)) is significantly below 0 (Fig. 4).

A series of population projection matrices, A_t, was constructed by augmenting the female transition probability matrix with elements describing reproduction[10] (see Methods). These matrices were used to calculate population growth rate, life expectancy and expected lifetime number of reproductive events experienced by a female.

The asymptotic population growth rate (λ) is given by the dominant eigenvalue of the population projection matrix. When $\lambda > 1$, the population is asymptotically growing; when $\lambda < 1$, the population is asymptotically declining. Therefore, λ is an important indicator of the status of a population. If we assume all demographic parameters have been constant from 1980 to 1995 (M_1), we find that $\lambda = 1.01$ (95% confidence interval = [1.00, 1.02]; the confidence interval was estimated using the estimated covariance of parameters by taking the inverse of the Hessian matrix[10]), suggesting a population increase of 1% per year, on average, between 1980 and 1995. However, time-specific asymptotic growth rates (λ_t)—calculated from the time-varying matrices A_t using model M_2—declined from $\lambda_{1980} = 1.03$ to $\lambda_{1995} = 0.98$ (Fig. 5c). Population growth rate declined below 1 at around 1992. If the 1995 population growth rate were maintained, the population would go extinct.

The decline in λ_t is the net result of all the changes in the vital rates (a collective term for transition, survival, fertility and mortality rates). We determined how much the decline in each vital rate contributed to the decline in λ_t, using a life table response experiment (LTRE) analysis[5,6]. This analysis decomposes the changes in λ_t into contributions from each entry in A_t. Figure 5d shows the sum of the contributions of all matrix entries involving each stage. The results of this analysis show that the decline in λ_t is caused mainly by the decline in the survival probability of mothers (Fig. 5d).

The life expectancy at birth is the mean age at which individuals born in a given year would die if conditions of that year were maintained. It can be calculated by treating the transition matrix as an absorbing Markov chain and calculating the mean time to absorption (that is, death)[5]. During the early 1980s, the life expectancy of females was twice that of males (Fig. 5a). This may be typical of large cetaceans. (Killer whales (*Orcinus orca*), for example, exhibit a similar difference in life expectancy between females and males[15].) Female life expectancy has declined from about 51.8 years in 1980 to about 14.5 years in 1995. Until recently, life expectancy of females has exceeded that of males, but that is no longer true owing to the reduced survival probability of females.

The expected number of reproductive events during a female's lifetime[5] has declined from about 5.27 in 1980 to about 1.26 in 1995 (Fig. 5b). A mature female could once expect to reproduce 6.48 times; that number is now about 1.80.

The growth rate projections in Fig. 5c are deterministic. The right whale population is small, however, and the population of any single stage is even smaller. Because of this, it has been suggested that population projections should include demographic stochasticity (chance fluctuations due to the random fates of a small number of individuals; see ref. 5). To evaluate the effect of demographic stochasticity, we transformed the matrix A_{1995} into a multitype branching process[5], and calculated the probability distribution of times to extinction (Fig. 6). We compared this distribution with the deterministic prediction obtained by using A_{1995} and defining extinction as the time when total population size reached 1 individual. For both calculations, we used an initial condition of 150 females distributed according to the stable stage distribution. This simulates the hypothetical situation in which the vital rates of 1995 remain constant and neither environmental trends nor environmental fluctuations affect them.

The mean time to extinction under demographic stochasticity is 208 years (similar to the estimate of 191 years in ref. 1). The deterministic time to extinction is 245 years. Thus demographic stochasticity reduces expected extinction time by 15%. Figure 6 gives the complete distribution of extinction times; there is a 5% chance of extinction within 130 years and a 25% chance of extinction within 165 years. These calculations exclude other factors such as continued declining survival trends, environmental stochasticity and Allee effects, all of which would hasten extinction. Thus the expected time of 208 years should be considered an upper bound.

Right whale conservation efforts are directed towards reducing mortality due to entanglement and ship collisions. Because the

© 2001 Macmillan Magazines Ltd

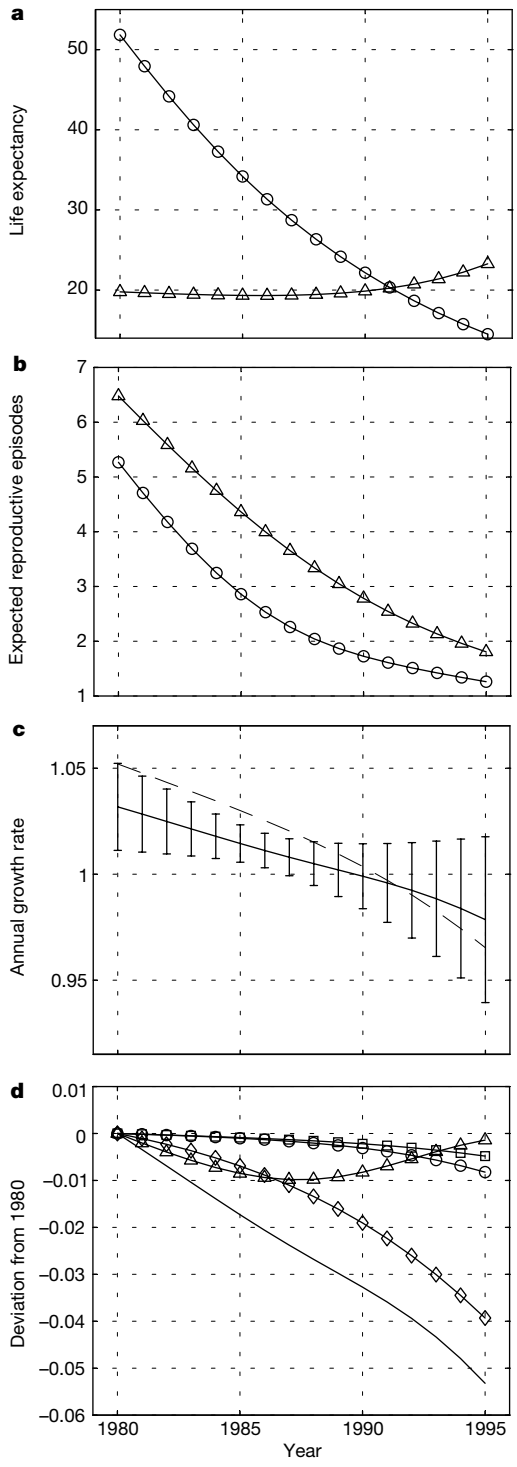

Figure 5 Demographic parameters calculated from the time-varying matrices A_t. **a**, The mean life expectancy at birth for males (triangles) and females (circles). **b**, The mean number of lifetime reproductive episodes, estimated from birth (circles) and from maturity (triangles). **c**, Asymptotic population growth rates λ_t (solid line) calculated from the population projection matrices A_t produced by the best model (M_2) and from the unstructured model of ref. 1 (dotted line). The error bars were standard errors, which were calculated using the series approximation to the variance of λ and the covariance matrix obtained from the information matrix. **d**, The result of a LTRE decomposition analysis for the trend in λ. The demographic rates in 1980 are used as the reference matrix, and the contributions of all matrix entries involving each stage were summed. The solid line shows the actual trend in λ, measured as a deviation from the value in 1980. It is closely approximated by the sum of all the other lines. Squares, calf; triangles, immature; circles, mature; diamonds, mothers.

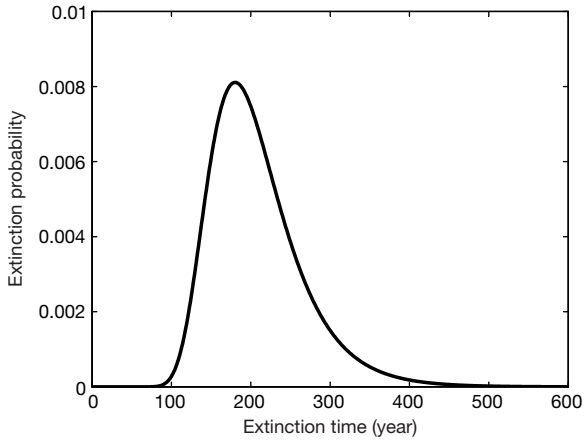

Figure 6 The probability distribution of time to extinction assuming demographic stochasticity. The distribution was calculated from a multi-type branching process, treating transitions and reproduction as independent events (multinomial and Bernoulli, respectively; see ref. 5).

population is so small, a single death represents a significant mortality rate. Conversely, significant reduction in mortality rate can be obtained by preventing just a few deaths. Figure 7 shows the effect on λ of preventing female deaths, using the vital rates of 1995 and assuming a starting population of 150 females distributed according to the stable stage distribution. The results indicate that prevention of just two female deaths every year would suffice to increase λ to 1. This gives a sense of the magnitude of the initial management action needed for the protection of the population. However, as population size increases owing to successful management, more deaths will have to be prevented to maintain a positive population growth rate because the number of deaths that translates into a given mortality rate also increases with the population size.

The causes behind the decline in survival probability of mothers are still unknown; however, collisions with ships, entanglement with fishing gear and changes in food availability due to climate fluctuations are suspected to contribute towards mortality[16,17]. Although right whales are distributed from the coast of northern Florida to the Bay of Fundy, it is primarily females and calves that are sighted in the calving ground off the coast of Florida and Georgia[18]. The calving ground is close to shipping lanes where large vessel traffic has increased since 1980 (ref. 19). More than 60% of North Atlantic right whales have scars from entanglement in fishing gear such as lobster pots and sink gillnets[17]. We have found a significant rank correlation between crude survival probability[1] (the survival probability of individuals without distinguishing stage differences) and North Atlantic Oscillation index (NAO), which is often used as an index for climate fluctuations[20]. Studies that focus on the effects of these three factors are urgently needed.

This study combines multi-stage mark–recapture methods and matrix population model analyses. Both methods incorporate differences in vital rates that are experienced by different stages within a population. Multi-stage mark–recapture analysis also incorporates stage-specific heterogeneity in sighting probability within the population. We succeeded in identifying a life cycle stage that is experiencing reduced survival probability, and were able to use the model to document the implications of that reduced survival probability for population growth.

Like any mark–recapture analysis, ours can be influenced by heterogeneity in sighting probability among individuals within a stage. If the sighting probability of mature females (stage 3) was heterogeneous, the survival probability of mothers towards the end of the study period would be underestimated. However, heterogeneity in sampling alone cannot explain the observed decline in the

© 2001 Macmillan Magazines Ltd

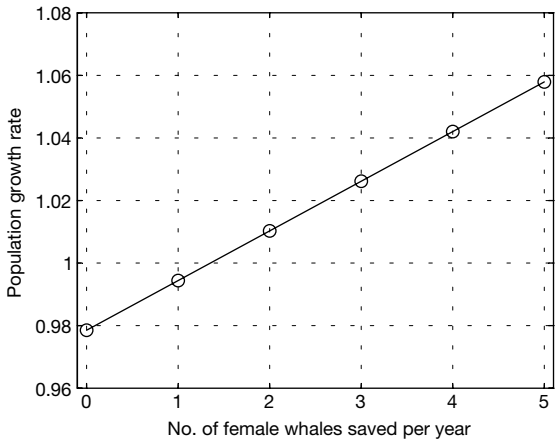

Figure 7 The predicted population growth rate that would result from preventing deaths of females regardless of their stage.

survival probability. Furthermore, during the winter of 1996, an unusually large number of confirmed mortalities were reported in the southeast United States, which is the only known calving ground[17]. This evidence suggests that the declining trend in the survival of mothers is both real and a great concern.

The North Atlantic right whale is currently seriously endangered owing to declining survival probability, especially among mothers. This finding, together with the unprecedented calf production in the spring of 2001 (ref. 21), suggests that Allee effects are not yet limiting this population. Our analysis also shows that the population was experiencing a positive growth rate in the early 1980s (Fig. 5c). This implies that it is not necessary to return the vital rates to those of the pre-whaling period to obtain a positive growth rate. There is every reason to hope that prompt management intervention can improve survival enough to permit the recovery of the North Atlantic right whale. □

Methods

Photographic identification data

Since 1980, the NEA has accumulated photographs of approximately 350 right whales taken on more than 10,000 sighting occasions. Individual right whales can be recognized by natural markings such as scars and callosity patterns. On the basis of these identifications the NEA has constructed a database of individual sighting histories, which consist of information on whether or not each individual was sighted at least once in each year. These data can be treated as if individuals were marked on the occasion of their first identifications, and recaptured at subsequent sightings. We used the data from 1980 to 1996, which were complete at the beginning of this analysis.

Statistical models

Sighting probabilities of each stage and transition probabilities among stages were estimated by fitting a series of statistical models to the sighting history data by maximum likelihood. The statistical models describe sighting probability as a function of sampling effort in two regions. The northern effort level is measured by the total annual survey days in Massachusetts Bay, Great South Channel, Bay of Fundy, and in Brown's Bank; the southern effort level is measured by the total annual survey days off the coast of Florida and Georgia. The dependence of sighting probability on the northern effort, the southern effort, both efforts, or neither effort was modelled with binary logistic functions. Let $s_i(t)$ be the sighting probability of stage i at time t. Then

$$s_i(t) = \frac{\exp(x_i + y_i e_{1,t} + z_i e_{2,t})}{1 + \exp(x_i + y_i e_{1,t} + z_i e_{2,t})} \quad (1)$$

where x_i is an intercept parameter, and y_i and z_i are slope parameters associated with northern ($e_{1,t}$) and southern ($e_{2,t}$) effort levels, respectively.

We modelled the transition probabilities of each stage as polychotomous logistic functions of time[10,22]. Let $p_{ji}(t)$ be the transition probability from stage i at time t to j at time $t+1$. Then

$$p_{ji}(t) = \frac{\exp(a_{ji} + b_{ji}t)}{1 + \sum_j \exp(a_{ji} + b_{ji}t)} \quad (2)$$

where a_{ji} and b_{ji} are intercept and slope parameters, respectively. When all the slope parameters are set to zero, the transition probabilities are time-invariant.

Model selection

Model selection was done in the following sequence. First, 1,024 sighting models were created by including all possible combinations of effort levels for all possible combinations of stages (equation (1)). These models were combined with the transition model in equation (2) in which all probabilities are functions of time. We selected the best of these models using AIC[12]. The AIC difference between the best and the second-best sighting models was about 2, indicating that the support for the best model relative to the second best model is high[14]. Therefore, we used only the best model. Because sighting probabilities of immature males and females did not differ significantly, by a likelihood ratio test, they were set equal. Using the resulting model for sighting, we selected the best time-varying transition matrix from all 64 models created by allowing the transition probabilities of all possible combination of stages to depend on time according to equation (2). The four best transition models had AIC differences from the best model of less than 2, indicating that the data provide some support for all these models. All of these models, however, had time-dependent survival probability of mothers.

Projection matrix

The projection matrix is

$$A_t = \begin{pmatrix} 0 & F_2 & F_3 & 0 \\ p_{21}(t) & p_{22}(t) & 0 & 0 \\ 0 & p_{32}(t) & p_{33}(t) & p_{34}(t) \\ 0 & p_{42}(t) & p_{43}(t) & 0 \end{pmatrix} \quad (3)$$

where

$$F_2 = 0.5 p_{42}(t) p_{34}^{0.5}(t+1) \quad (4)$$

and

$$F_3 = 0.5 p_{43}(t) p_{34}^{0.5}(t+1) \quad (5)$$

The first row of A_t describes reproduction; the other entries are transition probabilities. Consider F_2. When a female moves from stage 2 to stage 4 (with probability $p_{42}(t)$), she gives birth; the newborn calf is female with probability 0.5. Although newborn calves have distinct markings, they are harder to distinguish individually than other stages. Therefore, calf survival is estimated from the point where the calf is seen sufficiently well to permit identification, which is not necessarily on its first sighting. To appear as a calf in stage 1 at $t+1$, the newborn calf must survive long enough to be catalogued. We assume calves are catalogued on average midway through their first year, and that the mother must survive this long (with probability $p_{34}^{0.5}(t+1)$) in order for the calf to survive. F_3 is similar.

Received 18 May; accepted 21 September 2001.

1. Caswell, H., Fujiwara, M. & Brault, S. Declining survival probability threatens the North Atlantic right whale. *Proc. Natl Acad. Sci. USA* **96,** 3308–3313 (1999).
2. Knowlton, A. R., Kraus, S. D. & Kenney, R. D. Reproduction in North Atlantic right whales (*Eubalaena glacialis*). *Can. J. Zool.* **72,** 1297–1305 (1994).
3. Gerber, L. R., DeMaster, D. P. & Roberts, S. P. Measuring success in conservation. *Am. Sci.* **88,** 316–324 (2000).
4. Allee, W. C. *Animal Aggregations* (Univ. Chicago Press, Chicago, 1931).
5. Caswell, H. *Matrix Population Models: Construction, Analysis and Interpretation* 2nd edn (Sinauer Associates, Sunderland, Massachusetts, 2001).
6. Caswell, H. *Matrix Population Models* (Sinauer Associates, Sunderland, Massachusetts, 1989).
7. Tuljapurkar, S. & Caswell, H. *Structured-population Models in Marine, Terrestrial, and Freshwater Systems* (Chapman & Hall, New York, 1997).
8. Brault, S. & Caswell, H. Pod-specific demography of killer whales (*Orcinus orca*). *Ecology* **74,** 1444–1454 (1993).
9. Nichols, J. D., Sauer, J. R., Pollock, K. H. & Hestbeck, J. B. Estimating transition probabilities for stage-based population projection matrices using capture-recapture data. *Ecology* **73,** 306–312 (1992).
10. Fujiwara, M. & Caswell, H. Estimating population projection matrices from multi-stage mark-recapture data. *Ecology* (in the press).
11. Crone, M. J. & Kraus, S. D. *Right Whale (Eubalaena glacialis) in the Western North Atlantic: a Catalog of Identified Individuals* (New England Aquarium, Boston, Massachusetts, 1990).
12. Akaike, H. in *International Symposium on Information Theory* 2nd edn (eds Petran, B. N. & Csaki, F.) 267–281 (Akademiai Kiado, Budapest, 1973).
13. Lebreton, J.-D., Burnham, K. P., Clobert, J. & Anderson, D. R. Modeling survival and testing biological hypotheses using marked animals: a unified approach with case studies. *Ecol. Monogr.* **62,** 67–118 (1992).
14. Burnham, K. P. & Anderson, D. R. *Model Selection and Inference: a Practical Information-theoretic Approach* (Springer, New York, 1998).
15. Olesiuk, P. F., Bigg, M. A. & Ellis, G. M. in *Individual Recognition of Cetaceans: Use of Photo-identification and Other Techniques to Estimate Population Parameters* (eds Hammond, P. S., Mizroch, S. A. & Donovan, G. P.) 209–243 (Rep. Int. Whaling Comm. Special Issue 12, Cambridge, 1990).
16. Kraus, S. D. Rates and potential causes of mortality in North Atlantic right whales (*Eubalaena glacialis*). *Mar. Mamm. Sci.* **6,** 278–291 (1990).
17. Waring, G. T. *et al. U.S. Atlantic and Gulf of Mexico Marine Mammal Stock Assessments—1999.* NOAA Technical Memorandum NMFS-NE-153 (Northeast Fisheries Science Center, Woods Hole, Massachusetts, 1999).

© 2001 Macmillan Magazines Ltd

18. Kraus, S. D., Prescott, J. H., Knowlton, A. R. & Stone, G. S. in *Right Whale: Past and Present Status* (eds Brownell, R. L. Jr, Best, P. B. & Prescott, J. H.) 145–151 (Rep. Int. Whaling Comm. Special Issue 10, Cambridge, 1986).
19. Knowlton, A. R. in *Shipping/Right Whale Workshop* (eds Knowlton, A. R., Kraus, S. D., Meck, D. F. & Mooney-Seus, M. L.) 31–36 (New England Aquarium Aquatic Forum Series Report 97–3, Massachusetts, 1997).
20. Planque, B. & Reid, P. C. Predicting *Calanus finmarchicus* abundance from a climatic signal. *J. Mar. Biol. Ass. UK* **78,** 1015–1018 (1998).
21. Holden, C. Whale baby boomlet. *Science* **291,** 429 (2001).
22. Hosmer, D. W. & Lemeshow, D. *Applied Logistic Regression* (Wiley, New York, 1989).

Acknowledgements

We thank S. Kraus, A. Knowlton, P. Hamilton and the NEA for data. We also thank S. Brault, M. Hill, P. Kareiva, J.-D. Lebreton, M. Neubert, J. Nichols and the participants of the first Woods Hole Workshop on the Demography of Marine Mammals for discussions and suggestions. This project was funded by the Woods Hole Oceanographic Institution Sea Grant Program, the Rinehart Coastal Research Center, the David and Lucile Packard Foundation and The Robert W. Morse Chair.

Correspondence and requests for materials should be addressed to M.F. (e-mail: mfujiwara@whoi.edu).

Transgenic DNA introgressed into traditional maize landraces in Oaxaca, Mexico

David Quist & Ignacio H. Chapela

Department of Environmental Science, Policy and Management, University of California, Berkeley, California 94720-3110, USA

Concerns have been raised about the potential effects of transgenic introductions on the genetic diversity of crop landraces and wild relatives in areas of crop origin and diversification, as this diversity is considered essential for global food security. Direct effects on non-target species[1,2], and the possibility of unintentionally transferring traits of ecological relevance onto landraces and wild relatives have also been sources of concern[3,4]. The degree of genetic connectivity between industrial crops and their progenitors in landraces and wild relatives is a principal determinant of the evolutionary history of crops and agroecosystems throughout the world[5,6]. Recent introductions of transgenic DNA constructs into agricultural fields provide unique markers to measure such connectivity. For these reasons, the detection of transgenic DNA in crop landraces is of critical importance. Here we report the presence of introgressed transgenic DNA constructs in native maize landraces grown in remote mountains in Oaxaca, Mexico, part of the Mesoamerican centre of origin and diversification of this crop[7–9].

In October and November 2000 we sampled whole cobs of native, or 'criollo', landraces of maize from four standing fields in two locations of the Sierra Norte de Oaxaca in Southern Mexico (samples A1–A3 and B1–B3), more than 20 km from the main mountain-crossing road that connects the cities of Oaxaca and Tuxtepec in the Municipality of Ixtlán. As each kernel results from ovule fertilization by individual pollen grains, each pooled criollo sample represents a composite of ~150–400 pollination events. One additional bulk grain sample (K1) was obtained from the local stores of the Mexican governmental agency Diconsa (formerly the National Commission for Popular Subsistence), which distributes subsidized food throughout the country. Negative controls were cob samples of blue maize from the Cuzco Valley in Peru (P1) and a 20-seed sample from an historical collection obtained in the Sierra Norte de Oaxaca in 1971 (H1). Positive controls were bulk grain samples of Yieldgard *Bacillus thuringiensis* (Bt)-maize (Bt1; Monsanto Corporation) and Roundup-Ready maize (RR1; Monsanto Corporation) obtained from leftover stock for the 2000 planting season in the United States. Using a polymerase chain reaction (PCR)-based approach, we first tested for the presence of a common element in transgenic constructs currently on the market—the 35S promoter (p-35S) from the cauliflower mosaic virus (CMV). The high copy number and widespread use of p-35S in synthetic vectors used to incorporate transgenic DNA during plant transformation make it an ideal marker to detect transgenic constructs[10–12].

We obtained positive PCR amplification using primers specific for p-35S in five of the seven Mexican maize samples tested (Fig. 1). Four criollo samples showed weak albeit clear PCR amplification, whereas the Diconsa sample yielded very strong amplification comparable in intensity to transgenic-positive Bt1 and RR1 controls. The historical negative control (data not shown) and the contemporary sample from Cuzco, Peru, were both invariably negative. Low PCR amplification from landraces was due to low transgenic abundance (that is, a low percentage of kernels in each cob), not to differential efficiency in the reaction, as demonstrated by internal control amplification of the maize-specific alpha zein protein 1 gene (Fig. 1, *zp1*). During the review period of this manuscript, the Mexican Government (National Institute of Ecology, INE, and National Commission of Biodiversity, Conabio) established an independent research effort. Their results, published through official government press releases, confirm the presence of transgenic DNA in landrace genomes in two Mexican states, including Oaxaca. Samples obtained by the Mexican research initiative from sites located near our collection areas in the Sierra Norte de Oaxaca also confirm the relatively low abundance of transgenic DNA in these remote areas. The governmental research effort analysed individual kernels, making it possible for them to quantify abundances in the range of 3–10%. Because we pooled all kernels in each cob, we cannot make such a quantitative statement, although low PCR amplification signal from criollo samples is compatible with abundances in this percentage range.

Using a nested primer system, we were able to amplify the weak bands from all CMV-positive criollo samples (Fig. 1) sufficiently for nucleotide sequencing (GenBank accession numbers AF434747–AF434750), which always showed at least 98% homology with CMV p-35S constructs in commercially used vectors such as pMON273 (GenBank accession number X04879.1) and the K1 sample (accession number AF434746).

Further PCR testing of the same samples showed the presence of the nopaline synthase terminator sequence from *Agrobacterium tumefasciens* (T-NOS) in two of the six criollo samples (A3 and B2; GenBank accession numbers AF434752 and AF434751, respec-

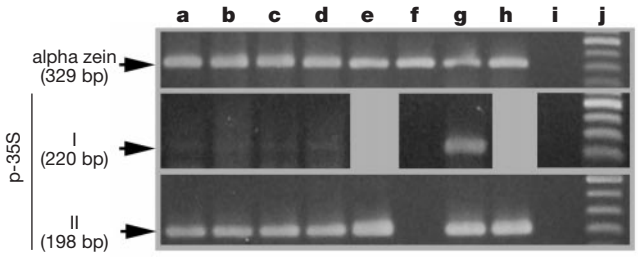

Figure 1 PCR amplification of DNA from the maize-specific alpha zein protein gene (top panel) and the CMV p-35S promoter (centre and bottom panels). The centre panel represents amplification protocol I (single amplification); the bottom panel indicates amplification protocol II (nested priming amplification). **a**–**d**, Criollo maize samples. Samples A2 (**a**), A3 (**b**), B2 (**c**) and B3 (**d**) are shown. **e**, Sample K1 from Diconsa store. **f**, Negative control P1, from Peru. **g**, Roundup-Ready maize RR1. **h**, Bt-maize Bt1. **i**, Internal negative control for PCR reaction. **j**, DNA ladder (100 base pairs (bp)), 500-bp marker at the top in each panel. Expected size for each fragment is marked on the left.

© 2001 Macmillan Magazines Ltd